Archaeometry Laboratory
University of Missouri Research Reactor

Investigations of Nasca-Wari Interactions and Imperial Expansion During the Wari Middle Horizon in the Nasca and Las Trancas Valleys, Nasca, Peru

FIRST REPORT

Prepared by:
William D. Gilstrap
Archaeometry Laboratory,
University of Missouri Research Reactor
Columbia, MO 65211

Prepared for:
Sarah Kerchusky
Department of Anthropology
University of California
Santa Barbara, CA 93106

October 04, 2016

Introduction

This report describes the preparation, analysis and interpretation of 75 pottery samples from three archaeological sites in the Sourthern Nasca Region (SNR) of Peru (Table 1). The study is part of an on-going project concerning ceramic production and exchange in the SNR during the Middle Horizon period (A.D. 750-1000). In this report compositional data obtained by neutron activation analysis (NAA) of Loro style pottery from the sites of Zorropata and Huaca del Loro of the Las Trancas Valley and Pataraya of the Tierras Blancas Valley in the SNR. This dataset is initially approached as a standalone project in attempts to identify and characterized discrete compositional groups at each site and then subsequently compared to previously analyzed SNR ceramics (i.e. Vaughn and Neff 2000, 2004; Vaughn et al. 2006). The specific goals of this study are to distinguish the potential for differences in production and vessel movement in Loro style pottery during this key period of the Wari Empire expansion to the south.

Here we describe sample preparation and analytical techniques used at MURR and report the subgroup structure identified through quantitative analysis of the compositional dataset and comparisons with previously analyzed samples from the region.

Sample Preparation

Specimens were prepared for INAA using procedures established at the Archaeometry Laboratory (Glascock 1992, Glascock and Neff 2003). Fragments of about $1cm^2$ were removed from each sherd and abraded using a silicon carbide burr in order to remove surface treatments (e.g., glaze, slip, paint) and adhering soil, thereby reducing the risk of measuring contamination. The specimens were washed in deionized water and allowed to dry in the laboratory. Once dry, the individual sherds were ground to powder in an agate mortar to homogenize them. Archival portions were retained from each sherd (when possible) for future research.

Two analytical samples were prepared from each specimen. Portions of approximately 150 mg of powder were weighed into high-density polyethylene vials used for short irradiations at MURR. At the same time, 200 mg aliquots from each sample were weighed into high-purity quartz vials used for long irradiations. Individual sample weights were recorded to the nearest 0.01 mg using an analytical balance. Both vials were sealed prior to irradiation. Along with the unknown samples, standards made from National Institute of Standards and Technology (NIST) certified standard reference materials of SRM-1633b (coal fly ash) and SRM-688 (basalt rock) were similarly prepared, as were quality control samples (e.g., standards treated as unknowns) of SRM-278 (obsidian rock) and Ohio Red Clay (a standard developed for in-house applications).

Irradiation and Gamma-Ray Spectroscopy

Procedures used for the irradiation and gamma-ray spectroscopy follow established MURR Archaeometry Laboratory protocol (Glascock 1992; Glascock and Neff 2003; Neff 2000). Neutron activation analysis of ceramics at MURR, which consists of two irradiations and a total of three gamma counts, constitutes a superset of the procedures used at most other NAA laboratories (Glascock 1992; Glascock and Neff 2003; Neff 2000). As discussed in detail by Glascock (1992), a short irradiation is carried out through the pneumatic tube irradiation system. Specimens in the polyvials are sequentially irradiated, two at a time, for five seconds by a neutron flux of 8×10^{13} n cm^{-2} s^{-1}. The 720-second count yields gamma spectra containing peaks for nine short-lived elements aluminum (Al), barium (Ba), calcium (Ca), dysprosium (Dy),

potassium (K), manganese (Mn), sodium (Na), titanium (Ti), and vanadium (V). The specimens are encapsulated in quartz vials and are subjected to a 24-hour irradiation at a neutron flux of 5×10^{13} n cm^{-2} s^{-1}. This long irradiation is analogous to the single irradiation utilized at most other laboratories. After the long irradiation, specimens decay for seven days, and then are counted for 1800 seconds (the "middle count") on a high-resolution germanium detector coupled to an automatic sample changer. The middle count yields determinations of seven medium half-life elements, namely arsenic (As), lanthanum (La), lutetium (Lu), neodymium (Nd), samarium (Sm), uranium (U), and ytterbium (Yb). After an additional three- or four-week decay, a final count of 8500 seconds is carried out on each specimen. The latter measurement yields the following 17 long half-life elements: cerium (Ce), cobalt (Co), chromium (Cr), cesium (Cs), europium (Eu), iron (Fe), hafnium (Hf), nickel (Ni), rubidium (Rb), antimony (Sb), scandium (Sc), strontium (Sr), tantalum (Ta), terbium (Tb), thorium (Th), zinc (Zn), and zirconium (Zr).

The element concentration data from the three measurements were tabulated in parts per million using Microsoft® Office Excel. Descriptive and contextual information for the specimens were appended to the spreadsheet of elemental abundances. These data are provided as an appendix to this report and as an accompanying digital file. Additional copies of these data are available upon request to the MURR Archaeometry Laboratory.

Interpreting Chemical Data

Analyses at MURR typically produce elemental concentration values for 33–34 elements. Some elements are present at or below the detection limits for neutron activation using current procedures. The element Ni was at or below detection limits in 107 specimens (89% of the sample). As such, we removed this element consideration in the analysis. Statistical analyses are carried out on base-10 logarithms of the remaining 32 elemental concentrations. Use of log concentrations rather than raw data compensates for differences in magnitude between the major elements, such as Na, and trace elements, such as the rare earth or lanthanide elements (REEs). Transformation to base-10 logarithms also yields a more normal distribution for many trace elements.

The interpretation of compositional data obtained from the analysis of archaeological materials is discussed in detail elsewhere (e.g., Baxter and Buck 2000; Bieber, et al. 1976; Bishop and Neff 1989; Glascock 1992; Harbottle 1976; Neff 2000) and will only be summarized here. The main goal of data analysis is to identify distinct homogeneous groups within the analytical database. Based on the provenance postulate of Weigand et al. (1977), different chemical groups may be assumed to represent geographically restricted sources. For lithic materials such as obsidian, basalt, and cryptocrystalline silicates (e.g., chert, flint, or jasper), raw material samples are frequently collected from known outcrops or secondary deposits and the compositional data obtained on the samples is used to define the source localities or boundaries. The locations of sources can also be inferred by comparing unknown specimens (i.e., ceramic artifacts) to knowns (i.e., clay samples) or by indirect methods such as the “criterion of abundance” (Bishop, et al. 1982) or by arguments based on geological and sedimentological characteristics (e.g., Steponaitis, et al. 1996). The ubiquity of ceramic raw materials usually makes it impossible to sample all potential “sources” intensively enough to create groups of knowns to which unknowns can be compared. Lithic sources tend to be more localized and compositionally homogeneous in the case of obsidian or compositionally heterogeneous as is the case for most cherts.

Compositional groups can be viewed as "centers of mass" in the compositional hyperspace described by the measured elemental data. Groups are characterized by the locations of their centroids and the unique relationships (i.e., correlations) between the elements. Decisions about whether to assign a specimen to a particular compositional group are based on the overall probability that the measured concentrations for the specimen could have been obtained from that group.

Initial hypotheses about source-related subgroups in the compositional data can be derived from non-compositional information (e.g., archaeological context, decorative attributes) or from application of various pattern-recognition techniques to multivariate chemical data. Some pattern recognition techniques used to investigate archaeological datasets are cluster analysis (CA), principal components analysis (PCA), and discriminant analysis (DA). Each of the techniques has its own advantages and disadvantages which may depend upon the types and quantity of data available for interpretation.

The variables (measured elements) in archaeological and geological datasets are often correlated and frequently large in number. This makes handling and interpreting patterns within the data difficult. Therefore, it is often useful to transform the original variables into a smaller set of uncorrelated variables in order to make data interpretation easier. Of the above-mentioned pattern recognition techniques, PCA is a technique that transforms from the data from the original correlated variables into uncorrelated variables most easily.

Principal components analysis creates a new set of reference axes arranged in decreasing order of variance subsumed. The individual PCs are linear combinations of the original variables. The data can be displayed on combinations of the new axes, just as they can be displayed on the original elemental concentration axes. PCA can be used in a pure pattern-recognition mode, e.g., to search for subgroups in an undifferentiated data set, or in a more evaluative mode, e.g., to assess the coherence of hypothetical groups suggested by other criteria. Generally, compositional differences between specimens can be expected to be larger for specimens in different groups than for specimens in the same group, and this implies that groups should be detectable as distinct areas of high point density on plots of the first few components.

Principal components analysis of chemical data is scale dependent, and analyses tend to be dominated by those elements or isotopes for which the concentrations are relatively large. As a result, standardization methods are common to most statistical packages. A common approach is to transform the data into logarithms (e.g., base 10). As an initial step in the PCA of most chemical data at MURR, the data are transformed into log concentrations to equalize the differences in variance between the major elements such as Al, Ca and Fe, on one hand and trace elements, such as the rare-earth elements (REEs), on the other hand. An additional advantage of the transformation is that it appears to produce more nearly normal distributions for the trace elements.

One frequently exploited strength of PCA, discussed by Baxter (1992), Baxter and Buck (2000), and Neff (1994; 2002), is that it can be applied as a simultaneous R- and Q-mode technique, with both variables (elements) and objects (individual analyzed samples) displayed on the same set of principal component reference axes. A plot using the first two principal components as axes is usually the best possible two-dimensional representation of the correlation or variance-

covariance structure within the data set. Small angles between the vectors from the origin to variable coordinates indicate strong positive correlation; angles at 90 degrees indicate no correlation; and angles close to 180 degrees indicate strong negative correlation. Likewise, a plot of sample coordinates on these same axes will be the best two-dimensional representation of Euclidean relations among the samples in log-concentration space (if the PCA was based on the variance-covariance matrix) or standardized log-concentration space (if the PCA was based on the correlation matrix). Displaying both objects and variables on the same plot makes it possible to observe the contributions of specific elements to group separation and to the distinctive shapes of the various groups. Such a plot is commonly referred to as a *biplot* in reference to the simultaneous plotting of objects and variables. The variable inter-relationships inferred from a biplot can be verified directly by inspecting bivariate elemental concentration plots.

Whether a group can be discriminated easily from other groups can be evaluated visually in two dimensions or statistically in multiple dimensions. A metric known as the Mahalanobis distance (or generalized distance) makes it possible to describe the separation between groups or between individual samples and groups on multiple dimensions. The Mahalanobis distance of a specimen from a group centroid (Bieber et al. 1976; Bishop and Neff 1989) is defined by:

$$D^2_{y,x} = [y - \bar{X}]^t \, I_x \, [y - \bar{X}]$$

where y is the $1 \times m$ array of logged elemental concentrations for the specimen of interest, x is the n × m data matrix of logged concentrations for the group to which the point is being compared with $\bar{X}$ being it 1 × m centroid, and I_x is the inverse of the $m \times m$ variance–covariance matrix of group x. Because Mahalanobis distance takes into account variances and covariances in the multivariate group it is analogous to expressing distance from a univariate mean in standard deviation units. Like standard deviation units, Mahalanobis distances can be converted into probabilities of group membership for individual specimens. For relatively small sample sizes, it is appropriate to base probabilities on Hotelling's T^2, which is the multivariate extension of the univariate Student's t.

When group sizes are small, Mahalanobis distance-based probabilities can fluctuate dramatically depending upon whether or not each specimen is assumed to be a member of the group to which it is being compared. Harbottle (1976) calls this phenomenon *stretchability* in reference to the tendency of an included specimen to stretch the group in the direction of its own location in elemental concentration space. This problem can be circumvented by cross-validation, that is, by removing each specimen from its presumed group before calculating its own probability of membership (Baxter 1994; Leese and Main 1994). This is a conservative approach to group evaluation that may sometimes exclude true group members.

Small sample and group sizes place further constraints on the use of Mahalanobis distance: with more elements than samples, the group variance-covariance matrix is singular thus rendering calculation of I_x (and D^2 itself) impossible. Therefore, the dimensionality of the groups must somehow be reduced. One approach would be to eliminate elements considered irrelevant or redundant. The problem with this approach is that the investigator's preconceptions about which elements should be discriminate may not be valid. It also squanders the main advantage of multielement analysis, namely the capability to measure a large number of elements. An alternative approach is to calculate Mahalanobis distances with the scores on principal

components extracted from the variance-covariance or correlation matrix for the complete data set. This approach entails only the assumption, entirely reasonable in light of the above discussion of PCA, that most group-separating differences should be visible on the first several PCs. Unless a data set is extremely complex, containing numerous distinct groups, using enough components to subsume at least 90% of the total variance in the data can be generally assumed to yield Mahalanobis distances that approximate Mahalanobis distances in full elemental concentration space.

Lastly, Mahalanobis distance calculations are also quite useful for handling missing data (Sayre 1975). When many specimens are analyzed for a large number of elements, it is almost certain that a few element concentrations will be missed for some of the specimens. This occurs most frequently when the concentration for an element is near the detection limit. Rather than eliminate the specimen or the element from consideration, it is possible to substitute a missing value by replacing it with a value that minimizes the Mahalanobis distance for the specimen from the group centroid. Thus, those few specimens which are missing a single concentration value can still be used in group calculations.

Results and Discussion

Before any statistical analysis could be performed it was necessary to remove the element Nickel (Ni) from the entire dataset as the majority of samples registered values lower than the limits of detection in our laboratory. With the removal of Ni, the dataset was evaluated for the total variation of each element by calculating a total variation matrix (Aichenson 1986; Buxeda i Garrigós1999; Buxeda i Garrigós et al. 2001; Buxeda i Garrigós and Kilikoglou 2003; Kilikoglou et al. 2007). A total variation matrix (TVM) is constructed of a table composed of log-transformed data where each element is expressed as a ratio of all other elements in the dataset (See Appendix II). Examination of the TVM has provided several pieces of key information for subsequent sample grouping and overall archaeological interpretation of the dataset. One of the main functions of the TVM is to demonstrate which variables (elements) have the most or least amount of variation within a dataset. In this case, the heavy metal arsenic (As) shows the most variation while cerium (Ce), a rare earth element, has the least amount of variation in the dataset. Arsenic is often a troublesome element in ceramic composition studies as it is easily absorbed from surrounding environments during the post-depositional phase of the object's history. Arsenic is often leached into sediments due to residues leftover from modern uses of agricultural pesticides and herbicides, or from metallurgical residues that occur due to mining, smelting or alloying (e.g. copper alloys). Eerkins et al. (2009) demonstrated that there are several areas in the SNR that show evidence of both modern and ancient metallurgical events thus shedding light on potential contaminate origins. In order to avoid any potential skewing of the data during the statistical investigations both As and antimony (Sb), an element often associated with As, have been removed from the dataset.

Second, the TVM has calculated a total variation (*vt*) value of 0.604. Total variation is the sum of all variances in the variation matrix divided by twice the number of elements in the matrix (Buxeda i Garrigós and Kilikoglou 2003:186). This value provides a metric to evaluate variability in a chemical dataset which is compatible with both variances and Euclidean distances (Schwalbe and Cuthbert 1988). This value is significant to the evaluation of ceramic composition studies as it is an indicator of what is referred to as monogenic or polygenic datasets. A low value indicates a monogenic dataset. For a study of ceramic composition, this translates to a

group made from chemically indiscrete raw materials (a group from a single origin). Polygenic datasets suggest that there is more than one discernable composition group in the dataset. Often the integer is equivalent to the amount of groups present in a single dataset, i.e. a *vt* value of 3.045 suggests that there are at least three compositionally discrete groups present in a dataset. The low *vt* value of 0.604 suggests that this dataset is monogenic or a single group made up of ceramic samples that derive from a single source.

With the removal of these problematic elements, the dataset was subjected to PCA. This test demonstrated that greater than 90% of the cumulative variance can be explained by the first 11 principal components (Table 2). Principal component (PC) 1 is only slightly positively loaded on the alkali elements Na and K while it has heavy negative loading on several elements including Mn, Co, Fe, Zn and V. The second component, PC 2 is positively loaded on Zr and negatively loaded on Cs. A biplot of these first two PCs displays the general structure of the dataset while accounting for over 45% of the cumulative variance (Figure 1). The structure illustrated by Figure 1 suggests that there two compositional groups with some outliers can be discriminated from the original dataset. This result is at odds from the results of the TVM described above perhaps suggesting that there are observable subgroups in a chemically similar dataset. In order to investigate this further, data were separated out according to archaeological site making it possible to see that each data cluster contains samples from all three sampled sites (Figure 2). Plotting the samples according to paste color (Figure 3) revealed little as nearly every paste color is represented in both clusters.

Data were then sorted according to inclusion grain size and replotted to reveal that those vessels containing coarse sand, medium coarse sand or medium sand are richer in alkali elements such as Na, K and Rb (Figure 4). Several samples with fine sand sized inclusions are mixed into this cluster which may suggest that the elemental spread in the data is derived from intrasource variability rather than inter-source variability. More plainly, the spread we see in these PCA biplots could be demonstrating the natural variability in the raw materials used by a single workshop or in a single raw material. The chemical spread may be due to the presence of certain mineral grains rich in alkali elements (Na, K, Rb) such as the alkali-feldspars present in granites, granodiorites, pegmatites and other acid igneous rocks, in the larger grain size fraction. Smaller mineral grains and rock fragments may have found their way into the fine fraction, thus explaining why we find only a few of these samples clustering with the more coarse varieties.

It is possible that all of the vessels sampled for this study derive from a common source and the small clustering visible in Figures 1-4, is due to the scale in which the samples are plotted. To test this, all samples were compared to a previous study of Middle Horizon polychrome pottery from the SNR region, including contemporary pottery from at Pecheco, Pataraya and Huaca del Loro with the addition of the upland site of Jincamocco in Ayacucho (Boulanger and Glascock 2012). The results of this earlier study demonstrated that polychrome pottery of various styles, including Loro and Wari-styles, sampled from the sites of Pataraya, Pacheco and Huaca del Loro were produced using chemically indistinct raw materials forming what they call *Group 1*. Only the vessels from Jincamocco were characterized as chemically distinct. *Group 1*, in this case, is chemically compatible with Vaughn et al.'s (2006; see also Vaughn and Neff 2000, 2004) *Group 1* which is composed of polychrome pottery from Early Nasca and Tiza cultures. Vaughn and his colleagues argue the production origin of this group to be at the ritual site of Cahuachi.

The resulting comparison demonstrates that both small clusters discussed above are chemically compatible with *Group 1* from the previous studies and is distinctive from Jincomocco pottery (Figure 5). Merging these samples with Vaughn's *Group 1* indicates that nearly all vessels in the current assemblage originate from a production a Cahuachi, or made with chemically indistinct raw materials as those used by Cahuachi based potters. Vaughn and Neff (2004: 1583) clearly demonstrate that while there are a large number of viable potting clays available in the SNR, however, these clay deposits are by no means homogeneous. The only clays chemically compatible with *Group 1* are in the lower valleys of the SNR, near the site of Cahuachi.

Preliminary Conclusions and Recommendations for Future Research

Chemical composition analysis of the Middle Horizon ceramic assemblages from three sites in the Southern Nasca Region are clear members of Vaughn's earlier *Group 1*. This result has provided new insight into a diachronic study of pottery production traditions and patterns of consumption in prehistoric southern Peru.

Previous studies have shown clear continuity exists in regional patterns of polychrome pottery production in the SNR between early Nasca and Tiza cultures. The present study provides new evidence of that production of polychrome and painted pottery at or near the site of Cahuachi is a tradition that moved through the Early Intermediate Period (ca. A.D. 1-750) *and* Middle Horizon (ca. A.D. 750-1000) and well into the Late Intermediate Period (ca. A.D. 1000-1476). This suggests that the potting tradition of Cahuachi-made polychrome and painted pottery is passed on for on for over 1400 years. It appears to start with the Nasca culture, continues with the Loro culture, is adopted by the Wari Empire during their southern expansion and continues into the Tiza culture that begins over 1000 years after the initial occurrence of this phenomenon.

Looking at a small subsample of such a large compositional group has enabled a glimpse into how variation in production technology of *Group 1* during the Middle Horizon period may affect compositional profiling. There appears to be a correlation between grain size fractions observed macroscopically and the abundance of alkali elements. Vessels that contain coarse and medium coarse sand sized inclusions show enrichment in elements, Na, K and Rb. These elements are from the alkali family and are constituent materials in the formation of alkali-feldspars. K and Na are commonly found in all varieties of alkali feldspars, orthoclase ([monoclinic], $KAlSi_3O_8$), sanidine ([monoclinic] $(K, Na)AlSi_3O_8$), microcline ([triclinic], $KAlSi_3O_8$) and anorthoclase ([triclinic], $(Na, K)AlSi_3O_8$). These minerals are often associated with acid-intermediate igneous rock such as granite and grano-diorite. Rb is often found as a replacement mineral for either K or Na in granitic pegmatites. In a small sample, the effect of the paste variation would have resulted in the separation of this larger group into subgroups. It may be useful to look into grain size distributions in future assessments of technological practice of Cahuachi potters over time to see if this pattern is significant archaeologically.

Looking now at the relationship between paste recipes with vessel shape and surface decoration, there seems to be little patter. The same paste recipe, as determined chemically, is used to form a wide variety of vessels shapes including bowls of varying types, ollas, jars and urns. The vessels can be painted or polychrome painted in Nasca, Loro, Wari or Tiza styles suggesting that while stylistic motifs change over time, the paste recipe stays the same. This is an interesting point for as Vaughn and Neff (2004:1580) point out, modern traditional potters from Nasca indicate that useable clay is available just outside their doorsteps. Such long term use of an unvarying paste

recipe suggests that the use of this recipe was significant to craftsmen at Cahuachi and perhaps reflective of the rituals that occurred there. This argument seems viable as these local craftsmen appear to have passed on specific information on how to prepare the paste for a Cahuachi polychrome pot for almost a millennium and a half. If this is the case it would stand to argue that the transmission of the technical information occurred probably vertically through the Nasca and perhaps into the Loro phases with the locus of replication situated in one-to-one familiar relationships, i.e. mother-daughter (Eerkins and Lipo 2007:251). During the expansion of the Wari Empire to the south and the subsequent occurrence of the Tiza culture, transmission of technical knowledge may hay shifted horizontally through what O'Brien and Lyman (2003) refer to as "hitchhikes" in which the technical knowledge may have been passed along as packages. Such a perspective is complementary to Katner and Vaughn's (2012) argument for continued religious pilgrimages to Cahuachi and the SNR over numerous generations in that it can be argued that the technical knowledge of producing ritual based ceramics was passed on along with other ritual/religious information that formed the foundation for the rites that occurred at the terminus point of the pilgrimage.

To understand the kinds of technological choices that occur with the production of such a culturally significant assemblage of pottery, it is suggested that the author or others initiate a technology-based study of the ceramic material from the early Nasca phase through to the end of the Tiza phases. In this way it will be possible to see if there is clear technological variation, including the use of different mixtures of similar raw materials over time. Mineralogical study of texturally distinct pastes (e.g. coarse sand vs very fine sand) by XRD or SEM in addition to thin section petrography may shed light as to what causes this chemical variation in the alkali elements.

Acknowledgments

Bianca Tomaszewski was responsible for preparation and irradiation of project specimens. This project was supported in part by NSF grant BCS-1659985 to the Archaeometry Laboratory of the Research Reactor, University of Missouri.

References

Aichenson, J.

1986 *The Statistical Analysis of Compositional Data.* Monographs on Statistics and Applied Probability. Chapman and Hall, Ney York.

Baxter, M. J.

1992 Archaeological Uses of the Biplot—A Neglected Technique? In *Computer Applications and Quantitative Methods in Archaeology, 1991*, edited by G. Lock and J. Moffett, pp. 141-148. BAR International Series. vol. S577. Tempvs Reparatvm, Oxford.

1994 *Exploratory Multivariate Analysis in Archaeology*. Edinburgh University Press, Edinburgh.

Baxter, M. J. and C. E. Buck

2000 Data Handling and Statistical Analysis. In *Modern Analytical Methods in Art and Archaeology*, edited by E. Ciliberto and G. Spoto, pp. 681-746. John Wiley and Sons, New York.

Bieber, A. M. J., D. W. Brooks, G. Harbottle and E. V. Sayre

1976 Application of Multivariate Techniques to Analytical Data on Aegean Ceramics. *Archaeometry* 18:59-74.

Bishop, R. L. and H. Neff

1989 Compositional Data Analysis in Archaeology. In *Archaeological Chemistry IV*, edited by R. O. Allen, pp. 576-586. Advances in Chemistry. vol. 220. American Chemical Society, Washington, D.C.

Bishop, R. L., R. L. Rands and G. R. Holley

1982 Ceramic Compositional Analysis in Archaeological Perspective. *Advances in Archaeological Method and Theory* 5:275-330.

Boulanger, M. T. and M. D. Glascock

2012 Inter-regional Interaction Between Sierra and Coast During the Wari Middle Horizon in Southern Ayacucho and Nasca. *Unpublished report.*

Buxeda i Garrigós, J.

1999 Alteration and Contamination of Archaeological Ceramics: The Perturbation Problem. *Journal of Archaeological Science* 26:295-313.

Buxeda i Garrigós, J., Cau Ontiveros, M. A. and V. Kilikoglou

2003 Chemical variability in Clays and Pottery from a Traditional Cooking Pot Village: Testing Assumptions in Pereruela. *Archaeometry* 45:1-17.

Buxeda i Garrigós, J. and V. Kilikoglou

2003 Total Variation as a Measure of Variability in Chemical Datasets. In *Patterns and Process, a Festschrist in Honor of Dr. Edward V. Sayre*, edited by L. Van Zelst. pp. 185-198. Smithsonian Center for Materials Research and Education: Washington D.C.

Buxeda i Garrigós, J., Kilikoglou, V. and P. M. Day
2001 Chemical and Mineralogical Alteration of Ceramics from a Late Bronze Age Kiln at Kommos, Crete: The Effect on the Formation of a Reference Group. *Archaeometry* 43:349-371.

Eerkins, J. W. and C. P. Lipo
2009 Cultural Transmission Theory and the Archaeological Record: Providing Context to Understanding Variation and Temporal Changes in Material Culture. *Jounral of Archaeological Research* 15:239-274.

Eerkins, J. W., Vaughn, K. J. and M. L. Grados
2009 Pre-Inca mining in the Southern Nasca Region, Peru. *Antiquity* 83:738-750.

Glascock, M. D.
1992 Characterization of Archaeological Ceramics at MURR by Neutron Activation Analysis and Multivariate Statistics. In *Chemical Characterization of Ceramic Pastes in Archaeology*, edited by H. Neff, pp. 11-26. Prehistory Press, Madison, WI.

Glascock, M. D. and H. Neff
2003 Neutron Activation Analysis and Provenance Research in Archaeology. *Measurement Science and Technology* 14:1516-1526.

Harbottle, G.
1976 Activation Analysis in Archaeology. *Radiochemistry* 3(1):33-72.

Katner, J. and K. J. Vaughn
2012 Pilgrimage as Costly Signal: Religiously Motivated Cooperation in Chaco and Nasca. *Journal of Anthropological Archaeology* 31:66-82.

Kilikoglou, V., Grimanis, A. P., Tsolakidou, A., Hein, A., Malamidou, D. and Z. Tsirtsoni
2007 Neutron Activation Patterning of Archaeological Materials at the National center for Scientific Research 'Demokritos': The Case of Black on red Neolithic Pottery from Macedonia, Greece. *Archaeometry* 49:301-319.

Leese, M. N. and P. L. Main
1994 The Efficient Computation of Unbiased Mahalanobis Distances and their Interpretation in Archaeometry. *Archaeometry* 36:307-316.

Neff, H.
1994 RQ-mode Principal Component Analysis of Ceramic Compositional Data. *Archaeometry* 36:115-130.

2000 Neutron Activation Analysis for Provenance Determination in Archaeology. In *Modern Analytical Methods in Art and Archaeology*, edited by E. Ciliberto and G. Spoto, pp. 81-134. John Wiley and Sons, New York.

2002 Quantitative Techniques for Analyzing Ceramic Compositional Data. In *Ceramic Source Determination in the Greater Southwest*, edited by D. M. Glowacki and H. Neff. Monograph 44. Cotsen Institute of Archaeology, Los Angeles.

Neff, H., R. L. Bishop, and E. V. Sayre

1988 A Simulation Approach to the Problem of Tempering in Compositional Studies of Archaeological Ceramics. *Journal of Archaeological Science* 15: 159-172.

1989 More Observations on the Problem of Tempering in Compositional Studies of Archaeological Ceramics. *Journal of Archaeological Science* 16: 57-69.

O'Brien, M. J. and R. L. Lyman

2003 Style, Function, Transmission: An Introduction. In *Style, Function, Transmission: Evolutionary Archaeological Perspectives*, edited by M. J. O'Brien and R. L. Lyman, pp. 1-32. University of Utah Press, Salt Lake City.

Rice, P. M.

1987 *Pottery Analysis: A Sourcebook*. University of Chicago Press, Chicago.

Sayre, E. V.

1975 *Brookhaven Procedures for Statistical Analyses of Multivariate Archaeometric Data*. Brookhaven National Laboratory Report BNL-23128.

Schwalbe, L. A. and T. P. Culbert

1988 Analytical Measures of Variability and Group Differences in X-Ray Fluorescence Data. *Journal of Archaeological Science* 15:669-681.

Steponaitis, V., M. J. Blackman and H. Neff

1996 Large-scale Compositional Patterns in the Chemical Composition of Mississippian Pottery. *American Antiquity* 61(3):555-572.

Vaughn, K. and H. Neff

2000 Moving Beyond Iconography: Neutron Activation Analysis of ceramics from Marcaya, Peru, an Early Nasca Domestic Site. *Journal of Field Archaeology* 27:75-90.

2004 Tracing the Clay Source of Nasca Polychrome Pottery: Results from a Prliminary Raw Materials Study. *Journal of Archaeological Science* 31:1577-1586.

Vaughn, K. J., C. A. Conlee, H. Neff, and K. Schreiber

2006 Ceramic Production in Ancient Nasca: Provenance Analysis of Pottery from the Early Nasca and Tiza Cultures through INAA. *Journal of Archaeological Science* 33: 681-689.

Weigand, P. C., G. Harbottle and E. V. Sayre

1977 Turquoise Sources and Source Analysis: Mesoamerica and the Southwestern U.S.A. In *Exchange Systems in Prehistory*, edited by T. K. Earle and J. E. Ericson, pp. 15-34. Academic Press, New York.

Table 1. Ceramic samples from three Middle Horizon sites reported in this study.

Site Name	Analytical IDs	n
Zorropata	MEP120–MEP173	53
Pataraya	MEP174–MEP184	11
Huaca del Loro	MEP185–MEP195	11
		Σ = 75

Table 2. Principal components analysis of the ceramic sample from SNR showing the first eleven components, describing greater than 90% of the cumulative variance in the dataset. Strong elemental loading along a particular component is indicated in bold.

Variable	PC1	PC2	PC3	PC4	PC5	PC6	PC7	PC8	PC9	PC10	PC11
% Variance	30.59	14.76	10.72	8.18	6.90	5.75	3.74	3.00	2.64	2.32	1.94
% Cum. Variance	30.59	45.35	56.07	64.25	71.15	76.90	80.64	83.63	86.28	88.60	90.54
Eigenvalues:	0.031	0.015	0.011	0.008	0.007	0.006	0.004	0.003	0.003	0.002	0.002
Na	**0.118**	0.129	-0.110	-0.025	-0.104	0.090	-0.245	-0.165	**0.245**	-0.157	-0.225
K	**0.117**	-0.116	-0.026	-0.004	**0.263**	**0.339**	-0.129	-0.359	0.089	**-0.396**	-0.279
Rb	0.049	-0.112	-0.054	0.120	**0.259**	0.049	0.176	-0.150	-0.074	-0.005	0.035
Ba	0.043	0.182	-0.262	0.169	-0.055	0.002	-0.026	-0.189	0.052	**0.578**	0.056
U	0.008	0.271	-0.298	-0.119	0.470	**-0.356**	-0.173	0.113	0.210	0.193	**-0.360**
Sr	-0.040	-0.099	**-0.389**	0.201	-0.226	-0.041	-0.219	**-0.300**	**-0.330**	-0.037	-0.261
Ca	-0.043	-0.110	**-0.353**	-0.274	**-0.417**	**-0.398**	-0.257	-0.063	-0.041	-0.245	0.255
Ta	-0.053	0.050	0.022	0.121	0.089	0.141	0.032	-0.008	-0.115	-0.043	0.107
Th	-0.073	0.217	-0.269	-0.062	0.458	0.114	**-0.313**	0.195	-0.212	-0.208	**0.460**
Al	-0.073	0.004	0.080	0.030	0.080	0.070	0.006	0.024	0.079	-0.002	-0.058
Lu	-0.089	0.116	0.094	-0.090	0.120	-0.246	-0.006	-0.095	0.055	-0.110	-0.145
La	-0.097	0.054	-0.007	0.074	0.117	-0.023	0.023	-0.156	-0.046	0.005	0.226
Ce	-0.115	0.024	-0.018	0.029	0.100	-0.015	-0.008	-0.155	-0.083	0.044	0.150
Yb	-0.132	0.155	0.108	-0.125	0.081	**-0.301**	0.177	-0.215	-0.029	0.017	0.081
Nd	-0.148	-0.012	0.123	0.060	0.091	-0.125	0.079	**-0.496**	0.006	0.025	0.172
Dy	-0.153	0.032	0.204	-0.006	0.041	-0.117	-0.082	-0.159	0.112	-0.089	-0.048
Sm	-0.154	0.037	0.093	0.011	0.069	-0.162	-0.042	-0.108	0.068	-0.038	0.085
Tb	-0.157	-0.081	0.137	0.028	0.084	-0.162	-0.064	-0.239	0.103	-0.147	0.033
Hf	-0.157	0.284	-0.184	0.181	-0.077	0.244	0.066	-0.172	-0.090	-0.114	-0.086
Eu	-0.179	-0.025	0.172	0.019	-0.061	-0.126	0.031	0.009	0.138	-0.115	0.058
Cr	**-0.208**	0.146	0.206	0.160	-0.032	0.081	-0.207	-0.080	**-0.439**	0.221	-0.007
Zr	**-0.231**	**0.501**	-0.195	0.168	-0.178	-0.058	**0.510**	0.127	0.015	**-0.295**	-0.134
Sc	**-0.234**	0.016	0.107	0.103	-0.016	-0.084	-0.170	0.068	-0.048	0.088	-0.088
Cs	**-0.240**	**-0.536**	**-0.359**	0.459	0.178	-0.126	0.208	0.128	0.191	-0.033	0.072
V	**-0.249**	0.179	0.043	0.218	-0.182	0.247	**-0.334**	0.081	0.523	-0.026	0.235
Zn	**-0.261**	-0.124	0.134	0.162	-0.025	-0.082	-0.239	0.099	0.047	0.161	-0.278
Fe	**-0.288**	0.005	0.059	0.036	-0.023	0.053	-0.127	0.193	-0.070	-0.081	-0.094
Co	**-0.309**	-0.132	0.057	-0.138	0.071	-0.009	-0.032	0.231	**-0.330**	-0.170	-0.228
Mn	**-0.484**	-0.151	-0.234	**-0.609**	-0.008	0.369	0.178	-0.129	0.126	**0.249**	-0.032

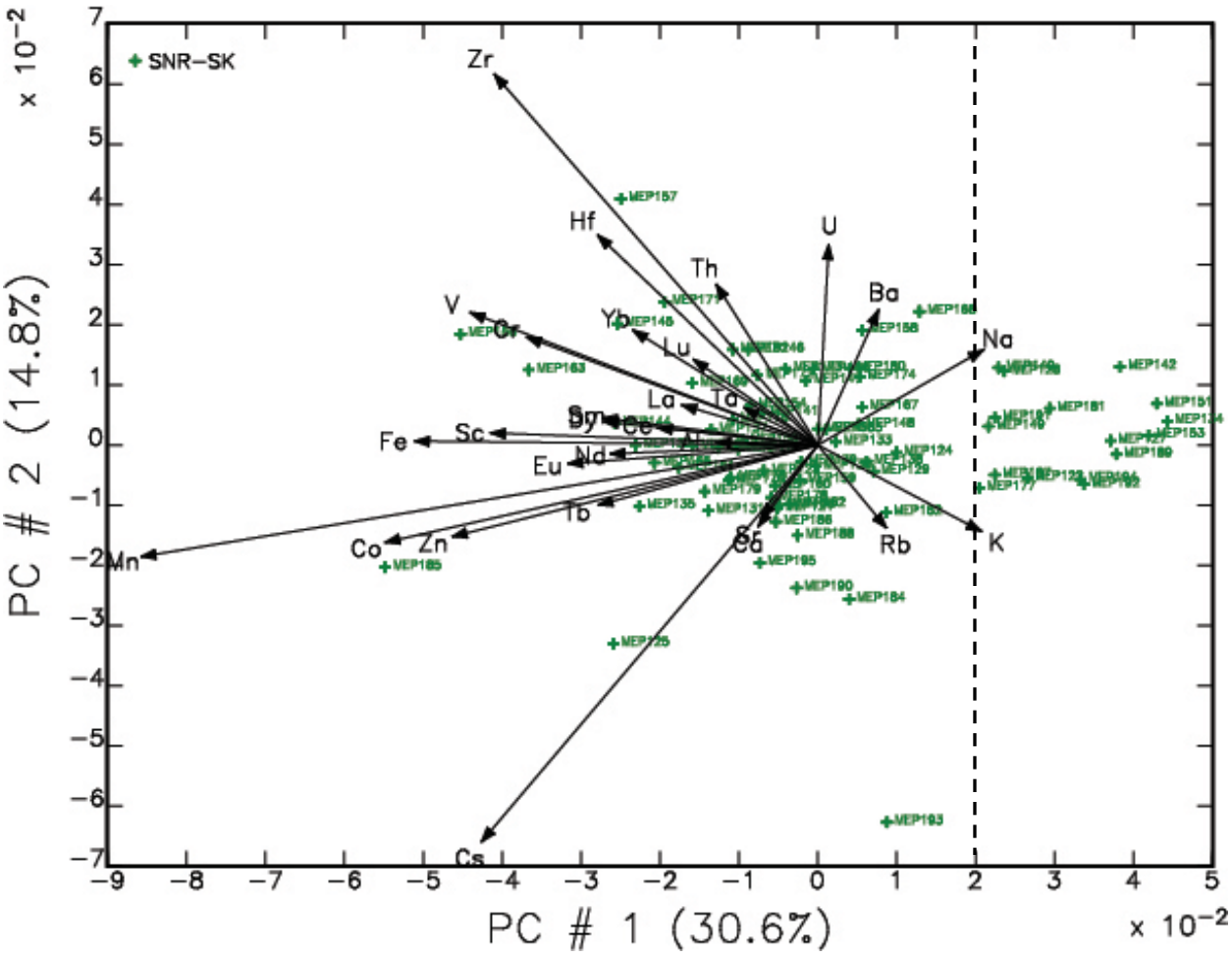

Figure 1. RQ-mode biplot of the first two principal components for the Middle Horizon Loro styleceramic sample from SNR. Loading vectors shown.

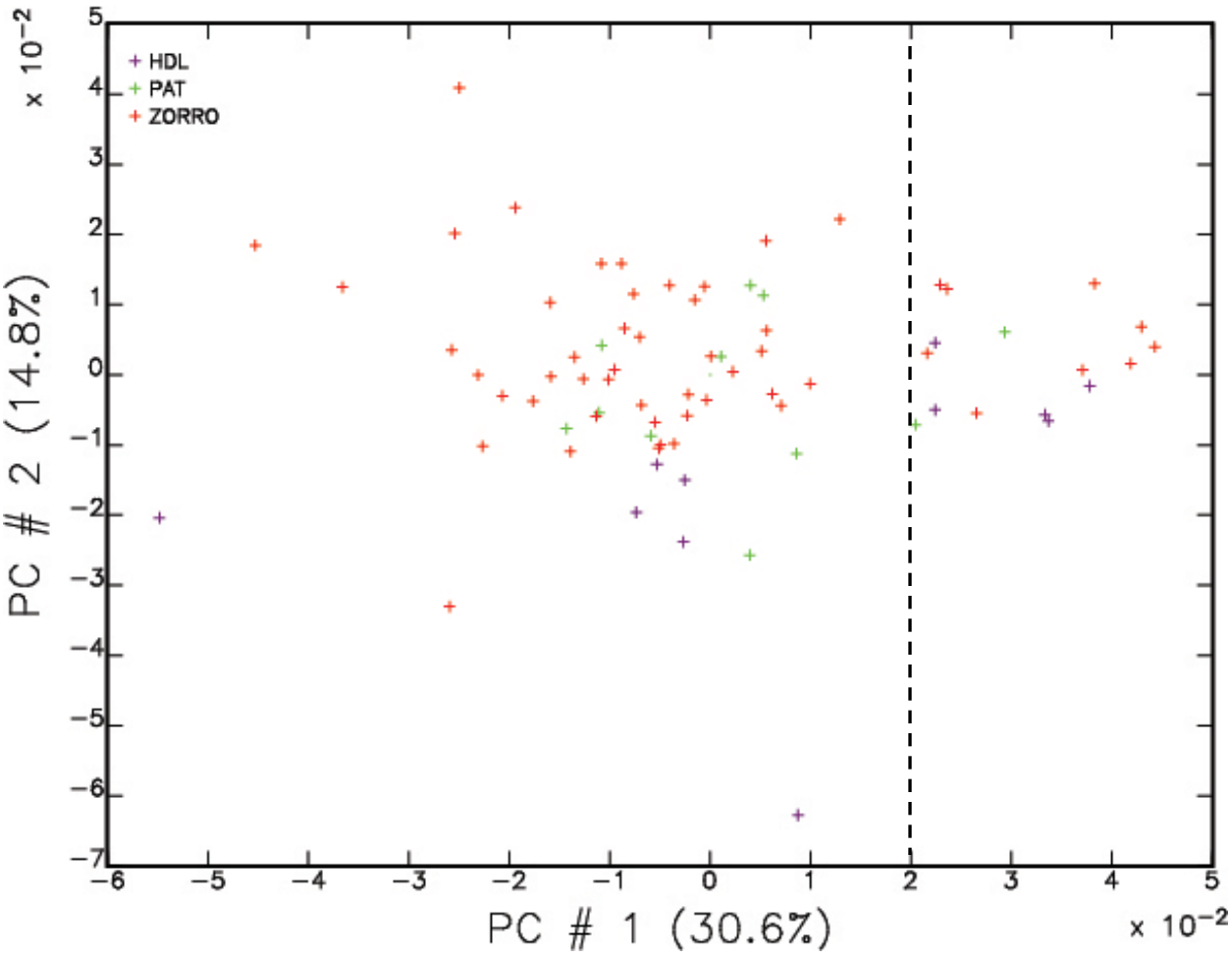

Figure 2. RQ-mode biplot of the first two principal components for the Middle Horizon Loro style ceramic sample from SNR. Data points are sorted according to site of depotisition: Huaco del Loro (HDL), Pataraya (PAT) and Zorrpata (ZORRO). Loading vectors not shown.

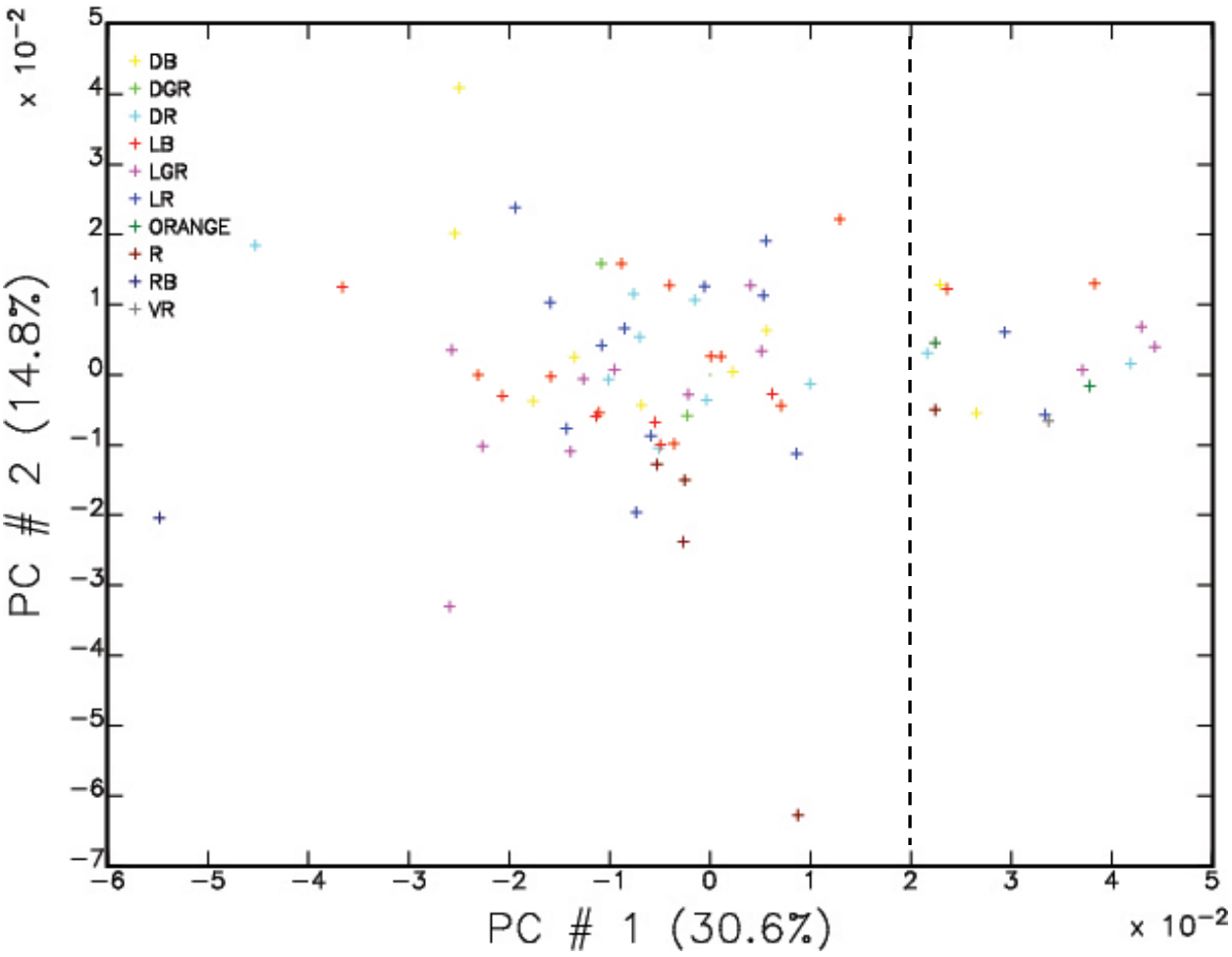

Figure 3. RQ-mode biplot of the first two principal components for the Middle Horizon Loro style ceramic sample from SNR. Datapoints are reflective of assigned paste color: dark brown (DB), dark grey red (DGR), dark red (DR), light brown (LB), light grey red (LGR), light red (LR), orange (ORANGE), red (R), red brown (RB) and very red (VR). Loading vectors not shown.

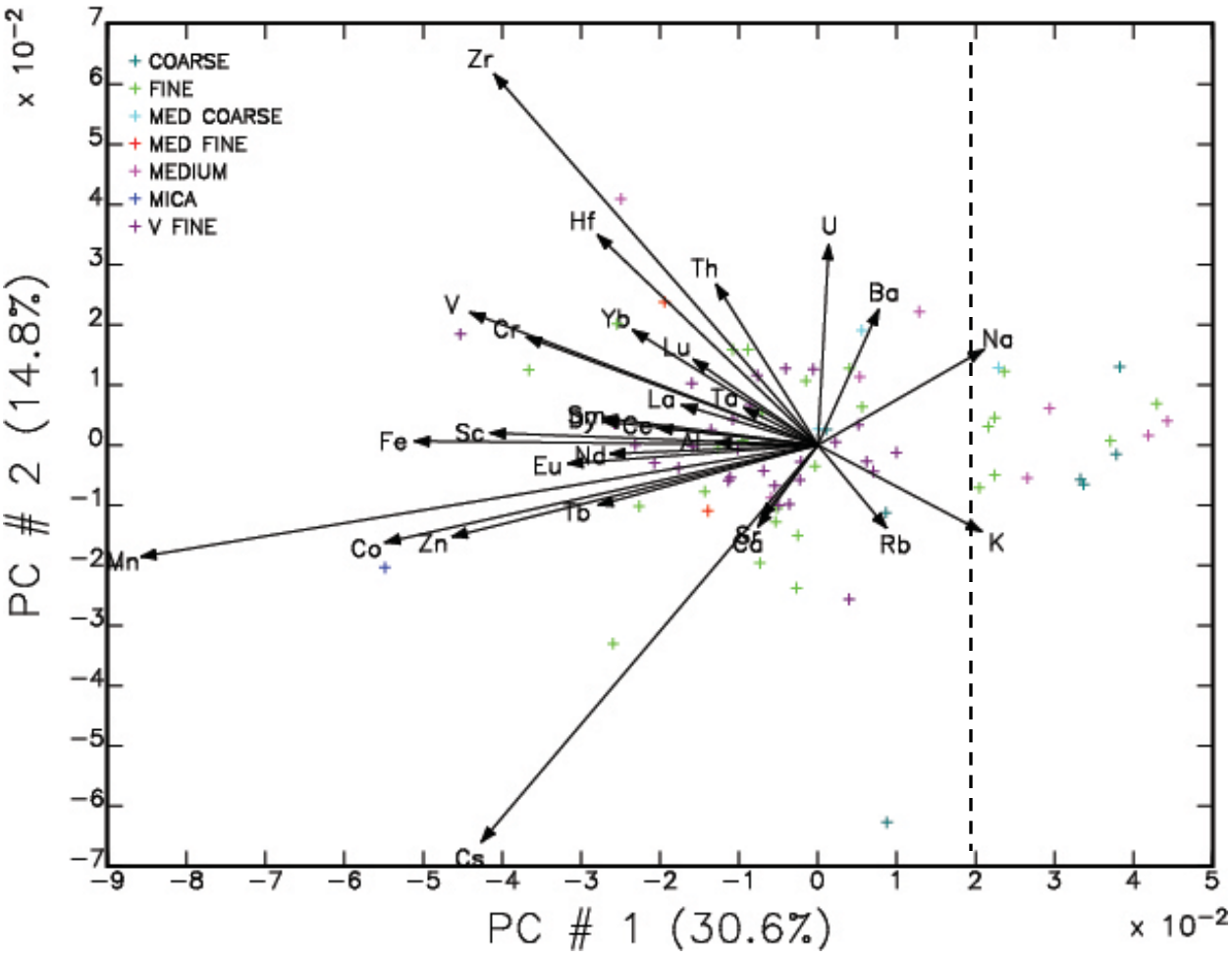

Figure 4. RQ-mode biplot of the first two principal components for the Middle Horizon Loro style ceramic sample from SNR. Data points are reflective of inclusion type and grain size: coarse sand, medium coarse sand, medium sand, medium fine sand, fine sand, very fine sand and mica. Loading vectors shown.

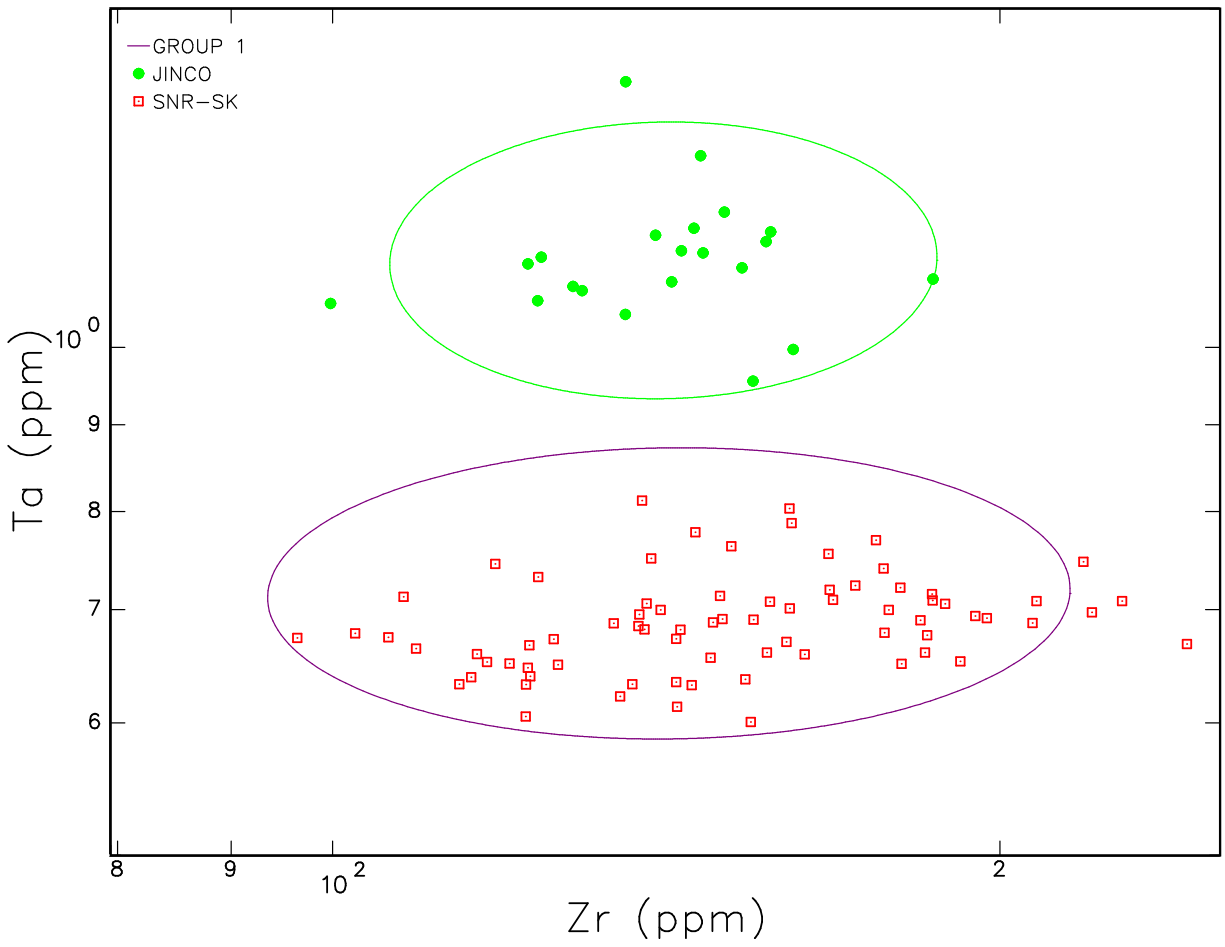

Figure 5: Elemental bivariate scatterplot comparing all samples from the current SNR datset to Vaughn et al.'s (2006) *Group 1* and pottery samples from Jincamocca in the Sondondo Valley of southern Ayacucho, Peru. Ellipses are drawn at 90%-confidence intervals.

Appendix I

Compositional and Descriptive Data for Middle Horizon Loro and Wari Ceramic Specimens from the Nasca and Las Trancas Valleys, Peru

Please see attached excel spreadsheet.

Appendix II

Total Variation Matrix for Middle Horizon Loro and Wari Ceramic Specimens from the Nasca and Las Trancas Valleys, Peru

	Na	Al	K	Ca	Sc	Ti	V	Cr	Mn	Fe	Co	Zn	As	Rb	Sr	Zr	Sb	Cs	Ba	La	Ce	Nd	Sm	Eu	Tb	Dy	Yb	Lu	Hf	Ta	Th	U
Na	0	0.017	0.023	0.037	0.033	0.043	0.038	0.04	0.094	0.038	0.052	0.044	0.177	0.024	0.025	0.053	0.039	0.084	0.019	0.019	0.02	0.031	0.024	0.03	0.029	0.026	0.032	0.021	0.027	0.018	0.033	0.033
Al	0.017	0	0.022	0.039	0.009	0.023	0.022	0.016	0.06	0.013	0.02	0.015	0.127	0.011	0.028	0.041	0.023	0.053	0.023	0.005	0.005	0.011	0.005	0.008	0.008	0.008	0.016	0.008	0.02	0.005	0.026	0.032
K	0.023	0.022	0	0.055	0.042	0.055	0.055	0.046	0.094	0.046	0.051	0.047	0.137	0.017	0.039	0.081	0.031	0.071	0.036	0.027	0.027	0.033	0.032	0.038	0.032	0.034	0.043	0.032	0.044	0.021	0.038	0.048
Ca	0.037	0.039	0.055	0	0.041	0.057	0.057	0.057	0.074	0.044	0.046	0.047	0.147	0.045	0.028	0.068	0.045	0.07	0.041	0.036	0.033	0.043	0.035	0.038	0.038	0.042	0.041	0.036	0.05	0.041	0.054	0.053
Sc	0.033	0.009	0.042	0.041	0	0.014	0.018	0.009	0.053	0.005	0.014	0.006	0.141	0.029	0.031	0.038	0.033	0.05	0.032	0.011	0.01	0.012	0.005	0.006	0.009	0.008	0.016	0.012	0.023	0.013	0.033	0.043
Ti	0.043	0.023	0.055	0.057	0.014	0	0.017	0.017	0.07	0.013	0.029	0.023	0.157	0.045	0.039	0.035	0.04	0.065	0.034	0.02	0.021	0.028	0.019	0.02	0.026	0.024	0.032	0.031	0.019	0.02	0.037	0.059
V	0.038	0.022	0.055	0.057	0.018	0.017	0	0.022	0.067	0.017	0.035	0.024	0.161	0.046	0.046	0.038	0.046	0.072	0.038	0.023	0.023	0.029	0.021	0.021	0.027	0.024	0.035	0.03	0.021	0.023	0.043	0.058
Cr	0.04	0.016	0.046	0.057	0.009	0.017	0.022	0	0.069	0.014	0.024	0.017	0.168	0.034	0.04	0.04	0.043	0.075	0.034	0.016	0.015	0.017	0.013	0.016	0.019	0.015	0.023	0.019	0.022	0.015	0.038	0.053
Mn	0.094	0.06	0.094	0.074	0.053	0.07	0.067	0.069	0	0.043	0.037	0.057	0.124	0.083	0.08	0.087	0.073	0.085	0.092	0.061	0.055	0.062	0.056	0.056	0.059	0.061	0.065	0.066	0.068	0.068	0.077	0.096
Fe	0.038	0.013	0.046	0.044	0.005	0.013	0.017	0.014	0.043	0	0.008	0.009	0.121	0.033	0.035	0.038	0.031	0.05	0.039	0.013	0.012	0.018	0.009	0.009	0.013	0.012	0.021	0.017	0.022	0.015	0.034	0.049
Co	0.052	0.02	0.051	0.046	0.014	0.029	0.035	0.024	0.037	0.008	0	0.016	0.097	0.036	0.042	0.056	0.031	0.05	0.055	0.022	0.018	0.024	0.017	0.016	0.018	0.019	0.027	0.023	0.036	0.024	0.043	0.056
Zn	0.044	0.015	0.047	0.047	0.006	0.023	0.024	0.017	0.057	0.009	0.016	0	0.133	0.031	0.037	0.055	0.039	0.043	0.042	0.018	0.016	0.019	0.012	0.012	0.013	0.013	0.027	0.021	0.034	0.02	0.048	0.055
As	0.177	0.127	0.137	0.147	0.141	0.157	0.161	0.168	0.124	0.121	0.097	0.133	0	0.124	0.159	0.195	0.09	0.104	0.191	0.131	0.127	0.136	0.134	0.13	0.119	0.14	0.146	0.141	0.152	0.127	0.158	0.177
Rb	0.024	0.011	0.017	0.045	0.029	0.045	0.046	0.034	0.083	0.033	0.036	0.031	0.124	0	0.028	0.061	0.017	0.047	0.025	0.011	0.011	0.02	0.018	0.024	0.019	0.022	0.029	0.02	0.031	0.011	0.032	0.035
Sr	0.025	0.028	0.039	0.028	0.031	0.039	0.046	0.04	0.08	0.035	0.042	0.037	0.159	0.028	0	0.057	0.029	0.046	0.024	0.024	0.023	0.033	0.029	0.034	0.031	0.037	0.043	0.034	0.029	0.025	0.043	0.049
Zr	0.053	0.041	0.081	0.068	0.038	0.035	0.038	0.04	0.087	0.038	0.056	0.055	0.195	0.061	0.057	0	0.063	0.102	0.042	0.036	0.038	0.047	0.037	0.041	0.051	0.044	0.037	0.037	0.021	0.038	0.049	0.053
Sb	0.039	0.023	0.031	0.045	0.033	0.04	0.046	0.043	0.073	0.031	0.031	0.039	0.09	0.017	0.029	0.063	0	0.03	0.035	0.02	0.019	0.032	0.028	0.032	0.028	0.036	0.042	0.033	0.033	0.018	0.033	0.044
Cs	0.084	0.053	0.071	0.07	0.05	0.065	0.072	0.075	0.085	0.05	0.05	0.043	0.104	0.047	0.046	0.102	0.03	0	0.072	0.051	0.05	0.054	0.053	0.052	0.048	0.062	0.075	0.068	0.074	0.054	0.078	0.09
Ba	0.019	0.023	0.036	0.041	0.032	0.034	0.038	0.034	0.092	0.039	0.055	0.042	0.191	0.025	0.024	0.042	0.035	0.072	0	0.019	0.02	0.031	0.026	0.034	0.035	0.032	0.03	0.027	0.023	0.019	0.032	0.03
La	0.019	0.005	0.027	0.036	0.011	0.02	0.023	0.016	0.061	0.013	0.022	0.018	0.131	0.011	0.024	0.036	0.02	0.051	0.019	0	0.001	0.008	0.004	0.01	0.008	0.009	0.014	0.009	0.016	0.005	0.021	0.029
Ce	0.02	0.005	0.027	0.033	0.01	0.021	0.023	0.015	0.055	0.012	0.018	0.016	0.127	0.011	0.023	0.038	0.019	0.05	0.02	0.001	0	0.008	0.004	0.01	0.008	0.009	0.013	0.009	0.017	0.006	0.022	0.03
Nd	0.031	0.011	0.033	0.043	0.012	0.028	0.029	0.017	0.062	0.018	0.024	0.019	0.136	0.02	0.033	0.047	0.032	0.054	0.031	0.008	0.008	0	0.006	0.011	0.008	0.01	0.014	0.012	0.027	0.013	0.038	0.043
Sm	0.024	0.005	0.032	0.035	0.005	0.019	0.021	0.013	0.056	0.009	0.017	0.012	0.134	0.018	0.029	0.037	0.028	0.053	0.026	0.004	0.004	0.006	0	0.003	0.004	0.004	0.009	0.005	0.021	0.009	0.027	0.032
Eu	0.03	0.008	0.038	0.038	0.006	0.02	0.021	0.016	0.056	0.009	0.016	0.012	0.13	0.024	0.034	0.041	0.032	0.052	0.034	0.01	0.01	0.011	0.003	0	0.006	0.006	0.014	0.009	0.028	0.013	0.039	0.046
Tb	0.029	0.008	0.032	0.038	0.009	0.026	0.027	0.019	0.059	0.013	0.018	0.013	0.119	0.019	0.031	0.051	0.028	0.048	0.035	0.008	0.008	0.008	0.004	0.006	0	0.007	0.015	0.009	0.029	0.012	0.037	0.042
Dy	0.026	0.008	0.034	0.042	0.008	0.024	0.024	0.015	0.061	0.012	0.019	0.013	0.14	0.022	0.037	0.044	0.036	0.062	0.032	0.009	0.009	0.01	0.004	0.006	0.007	0	0.012	0.008	0.026	0.012	0.035	0.041
Yb	0.032	0.016	0.043	0.041	0.016	0.032	0.035	0.023	0.065	0.021	0.027	0.027	0.146	0.029	0.043	0.037	0.042	0.075	0.03	0.014	0.013	0.014	0.009	0.014	0.015	0.012	0	0.008	0.028	0.017	0.034	0.033
Lu	0.021	0.008	0.032	0.036	0.012	0.031	0.03	0.019	0.066	0.017	0.023	0.021	0.141	0.02	0.034	0.037	0.033	0.068	0.027	0.009	0.009	0.012	0.005	0.009	0.009	0.008	0.008	0	0.024	0.012	0.027	0.024
Hf	0.027	0.02	0.044	0.05	0.023	0.019	0.021	0.022	0.068	0.022	0.036	0.034	0.152	0.031	0.029	0.021	0.033	0.074	0.023	0.016	0.017	0.027	0.021	0.028	0.029	0.026	0.028	0.024	0	0.014	0.03	0.04
Ta	0.018	0.005	0.021	0.041	0.013	0.02	0.023	0.015	0.068	0.015	0.024	0.02	0.127	0.011	0.025	0.038	0.018	0.054	0.019	0.005	0.006	0.013	0.009	0.013	0.012	0.012	0.017	0.012	0.014	0	0.022	0.034
Th	0.033	0.026	0.038	0.054	0.033	0.037	0.043	0.038	0.077	0.034	0.043	0.048	0.158	0.032	0.043	0.049	0.033	0.078	0.032	0.021	0.022	0.038	0.027	0.039	0.037	0.035	0.034	0.027	0.03	0.022	0	0.024
U	0.033	0.032	0.048	0.053	0.043	0.059	0.058	0.053	0.096	0.049	0.056	0.055	0.177	0.035	0.049	0.053	0.044	0.09	0.03	0.029	0.03	0.043	0.032	0.046	0.042	0.041	0.033	0.024	0.04	0.034	0.024	0
$\tau_{.1}$	1.223	0.718	1.397	1.536	0.799	1.133	1.197	1.044	2.191	0.84	1.045	0.994	4.373	1.018	1.248	1.68	1.134	1.978	1.23	0.696	0.681	0.878	0.7	0.813	0.81	0.839	0.993	0.831	1.051	0.744	1.285	1.528
$vt/\tau_{.1}$	0.493	0.841	0.432	0.393	0.755	0.533	0.504	0.578	0.275	0.718	0.578	0.607	0.138	0.593	0.484	0.359	0.532	0.305	0.491	0.867	0.887	0.687	0.862	0.742	0.745	0.719	0.608	0.726	0.574	0.811	0.47	0.395
r.vt	0.907	0.991	0.839	0.836	0.97	0.931	0.93	0.966	0.445	0.931	0.821	0.93	-0.528	0.899	0.891	0.851	0.771	0.428	0.908	0.994	0.997	0.983	0.991	0.973	0.971	0.98	0.962	0.975	0.927	0.982	0.901	0.856
vt	0.604																															